Physica Scripta. Vol. T73, 114–118, 1997

Recombination Studies of Highly Charged Ions in the Cooler Ring CRYRING

R. Schuch, D. R. DeWitt, H. Gao, S. Mannervik and W. Zong

Department of Atomic Physics, Stockholm University, S-104 05 Stockholm, Sweden

and

N. R. Badnell

Department of Physics, University of Strathclyde, Glasgow G4 0NG, U.K.

Received October 30, 1996; accepted in revised form January 22, 1997

Abstract

Cooler-storage ring facilities offer unique experimental possibilities for studies of electron-ion recombination processes at low relative energies by employing the electron cooler as a target. Through the use of an adiabatically expanded electron beam in the cooler of CRYRING, collisions down to 10^{-4} eV relative energies were measured with highly charged ions stored in the ring at around 15 MeV/amu energies. Examples of recombination measurements for C^{4+} and Ar^{15+} ions at an energy resolution of as low as 10^{-2} eV FWHM are presented and compared with calculations of the energies and resonance strength for dielectronic recombination using multiconfiguration Breit–Pauli approximations. They agree in spectral shape and absolute cross section but show some deviation for lower n in the Rydberg series.

1. Introduction

Electron cooling in storage rings opened up new possibilities to measure electron-impact ionization and recombination with unprecendented resolution and luminosity [1]. A number of interesting phenomena appear in these studies with important applications in fusion and astrophysical plasmas [2, 3] and fundamental atomic spectroscopy [4–8]. The following basic processes of recombination are distinguished:

$$A^{q+} + e^- \rightarrow A^{(q-1)+}(n) + h\nu. \quad (1)$$

$$+ e^- \rightarrow A^{(q-1)+}(n, n') \rightarrow A^{(q-1)+}(n) + h\nu, \quad (q < Z). \quad (2)$$

$$+ 2e^- \rightarrow A^{(q-1)+}(n) + e^-, \quad (3)$$

where Z is the nuclear charge and q is the charge state.

In process (1), radiative recombination (RR), a free electron is captured simultaneously with the emission of a photon into the quantum state n of ion $A^{(q-1)}$. It is the most fundamental process in the interaction of free electrons with ions. The RR cross section diverges for zero relative energies [9]. It is therefore the key process for lifetimes of stored beams during cooling with electrons in storage rings and is often used as a diagnostic tool for electron cooling.

In process (2), dielectronic recombination (DR), a free electron is captured simultaneously with the excitation of a bound electron in the projectile. Due to energy conservation, the binding energy plus the kinetic energy of the captured electron must equal the excitation energy of the bound electron. The resulting doubly excited state (n, n') will have a very large probability to autoionize and loose the electron again. It may, instead emit a photon and end up in a singly excited state. This last step completes dielectronic recombination. In studies of dielectronic recombination one can obtain accurate data on transition and binding energies, autoionization and radiative rates of singly resolved states in few-electron atomic systems which can serve to test atomic structure calculations [4, 6, 8].

In three-body recombination [TBR, process (3)] one electron recombines in the vicinity of another electron by transfering energy and momentum to it [10]. TBR can be viewed as the time reverse of electron-impact ionization; RR and the first step of DR is the time reverse of photoionization and of the Auger effect, respectively. Due to its dependence on the electron temperature and density, TBR can play an important role for the recombination rate in cold, dense electron plasma.

Recombination studies for bare ions (where in principle only RR and TBR can occur) for D^+, He^{2+}, N^{7+}, Ne^{10+} and Si^{14+} were done at CRYRING. The deuterons [11–13] have shown reasonably good agreement with RR predictions [9], however, increasing deviations are found for heavier ions [14–16] when compared to radiative recombination theory. In some cases of non-bare heavy ions deviations from RR theory by one to two orders of magnitude have been reported [17–19]. When cooling lead ions of a charge varying between $q = 52+$ and $54+$ the beam lifetime due to recombination changed by one to two orders of magnitude [20]. In recent case studies with Ar^{13+} and Au^{49-51+} DR resonances at very low relative energy ($E \leqslant 10$ meV) were identified to cause an increased rate for electron–ion recombination [18, 19]. With bare ions, however, an enhancement by DR is excluded. The enhancement factor varies from 60% for He^{2+} up to a factor of 3 for Si^{14+} of the RR rates. There are models which suggest that this could be caused by distortions of the free-electron continuum by e.g. Debye screening of the ion charge or by radiative stabilization of high-n states populated by three-body recombination [16]. It has also been proposed that it could be caused by external fields in the interaction region [21].

As examples for recombination measurements we report here a comparison of measured recombination rates with calculated dielectronic recombination rates for He-like C and Li-like Ar. We will also show a comparison of calculated RR with the measured rates for Ar^{15+} in a regime of relative energies where no DR resonances are expected. The DR cross sections are calculated in isolated resonance

approximation, using the AUTOSTRUCTURE code [22]. For center-of-mass (CM) energies (E_{cm}) of the first $\Delta n = 0$ transitions at around 1 eV in Ar^{14+} the resonance energies are determined with about 0.01 eV accuracy and 0.02 eV resolution. For $\Delta n = 1$ transitions at E_{cm} around 250 eV studied with He-like C the resolution is worse, but still the energies are measured with better than 0.1 eV accuracy. The absolute rates are determined to better than 30%. Measurement of these cross sections have also been done previously [5, 23]. With the accuracy reached in the present experiments a more crucial test of calculations of the energies and resonance strength should be possible.

2. Experiment

The experiments were performed at the ion storage ring CRYRING at the Manne Siegbahn Laboratory. The C^{4+} and Ar^{15+} ions, produced from an electron-beam ion source (CRYSIS), were injected into the ring at 300 keV/amu via an RFQ and accelerated to typically 13 MeV/amu after storage. In the experiments, about 10^6 heavy ions were stored in the ring. During electron cooling, the ions were merged over an effective interaction length of $l = 0.8$ m with a velocity matched electron beam, confined by a solenoid magnetic field of 0.03 T to a diameter of 40 mm, having a typical density of about $n_e = 2 \times 10^7\,\mathrm{cm}^{-3}$. Using the expanded electron beam of the electron cooler [24] very low electron beam temperatures could be reached for the measurements. The temperatures of the electron beam of $T_\perp = 10\,\mathrm{meV}/k_B$ and $T_\parallel = 0.1\,\mathrm{meV}/k_B$ were determined by cooling force measurements. From fitting DR resonances we find electron beam temperature transverse ($T_\perp$) and longitudinal ($T_\parallel$) components varying between 10 and 20 meV/k_B and 0.1 and 0.15 meV/k_B, respectively, depending on the adjustment of the electron beam relative to the ion beam. In the measurement with Ar^{15+} ions we had $T_\perp = 20\,\mathrm{meV}/k_B$ because of a displacement of the ion beam relative to the center of the electron beam (see below).

The recombined ions, formed in the cooler, are separated from the circulating beam in the first bending magnet downstream from the cooler, and are detected by a surface barrier detector inserted on a manipulator. The small separation between Ar^{15+} and Ar^{14+} ions required a displacement of the ion beam relative to the center of the electron beam in order to detect Ar^{14+}. As the recombined ions pass through the bending magnet, electrons bound above a certain n-level given by

$$n > n_{max} = \sqrt[4]{\frac{6.2 \times 10^8 q^3}{v_i B}}$$

are stripped by the motional electric field in the bending magnet. For our case we get from this relation $n_{max} = 43$ for Ar^{15+} ions and $n_{max} = 16$ for C^{4+} ions. After cooling the beam for typically 3 s, the relative velocity between the ion and electron beam is tuned through the resonances. The rate coefficients are determined in the experiments by

$$\alpha^{expt.} = \frac{\gamma^2 R^{det}}{n_e N_i}\left(\frac{L}{l}\right)$$

where γ is the Lorentz factor, R^{det} is the background corrected counting rate of recombined ions, N_i is the number of ions stored in the ring, and L is the ring circumference. At a vacuum of 10^{-11} Torr, the electron capture background is in the percent level of the total detected charge exchanged particles under cooling conditions. Most of the systematic experimental uncertainties are from the ion beam current measurement, which is estimated to be about 30%. Details of the experiment are described elsewhere [6].

After cooling the ion beam with the velocity matched electron beam, $[E_e = E_i(m_e/m_i)]$, the electron energy is changed by a certain amount ΔE_e which results in a CM energy (in nonrelativistic approximation): $E_{cm} = (\sqrt{E_e} \pm \sqrt{\Delta E_e})^2$. That small collision energies can be measured with high resolution as can be seen from the example: If a 12 keV electron beam (for cooling a 20 MeV/amu ion beam) is detuned by $\Delta E_e = 500$ eV, the resulting collision energy is only about 3 eV. Here we present one set of data where E_{cm} varies from 10^{-4} to around 30 eV and one set where it varies from 220 eV to around 320 eV.

The energy resolution that can be achieved in such measurements is limited by the energy spread of the electron beam, and the lateral spread of the ion beam in the space charge distribution of the electron beam. Due to the mass difference the velocity spread of the ion beam is small compared to that of the electron beam. At small collision energies the transverse energy spread of the electrons will usually dominate since it remains unaffected by the transformation to the center-of-mass system. With the expanded electron beam one gets an energy resolution of δE_{cm} around 0.01 eV below 1 eV collision energies and above this energy the resolution is determined to a larger extent by the longitudinal temperature of $T_\parallel \simeq 10^{-4}$ eV, through the relation $\delta E_{cm} = k_B T_\perp + k_B T_\parallel + 2\sqrt{E_{cm} k_B T_\parallel}$. A value of roughly 0.5 eV is obtained at around 200 eV CM energies (see below).

Scanning the electron beam at small detuning velocities, introduces a strong drag force on the ions. This drag force is due to repeated long range Coulomb collisions between electrons and ions and increases with ion charge and decreasing electron temperature. It has a disturbing effect on the transformation from laboratory to CM energies. For its correction, we have calculated the change of the velocity of the ions as a function of time during the scans by numerical solution of the differential equation describing the beam acceleration due to repeated Coulomb collisions in the electron beam (for details see Ref. [6]).

The drag force correction and the space-charge uncertainties in the electron beam seem to be the major obstacles in obtaining accurate resonance energies in such DR measurements. Therefore a new calibration method was developed [25] which takes care of most of the space-charge uncertainties. For calibration we ran the following cycles: After cooling the ions and reading the Schottky frequency, the cooler was set to a DR resonance energy and the ion beam was then accelerated or decelerated and cooled at this energy. Then the Schottky signal was analysed again and the trajectory of the ions determined by scrapers, i.e. the electrons velocity change is infered from a frequency difference. The main source of inaccuracy in this procedure comes from an uncertainty in the trajectory of the ions being cooled at the two different cooling energies. This enters when transforming from the Schottky frequencies to the matched ion and electron velocity. For details see Ref. [26].

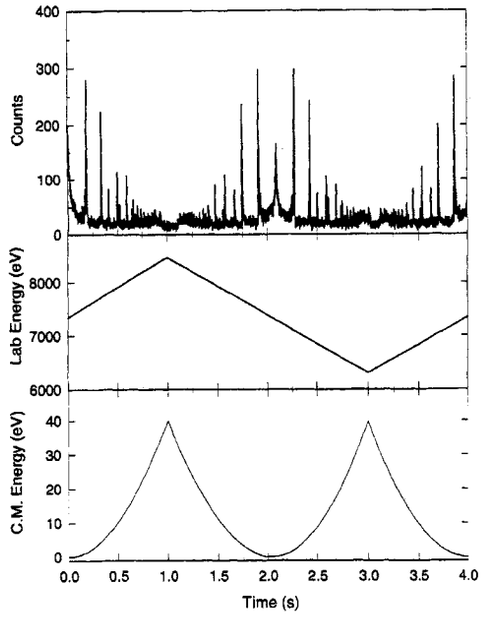

Fig. 1. Scans of the recombination rates for the stored lithium-like Ar ions. Top: counts of recombined ions, middle: variation of cathode voltage, bottom: CM energy as function of scanning time.

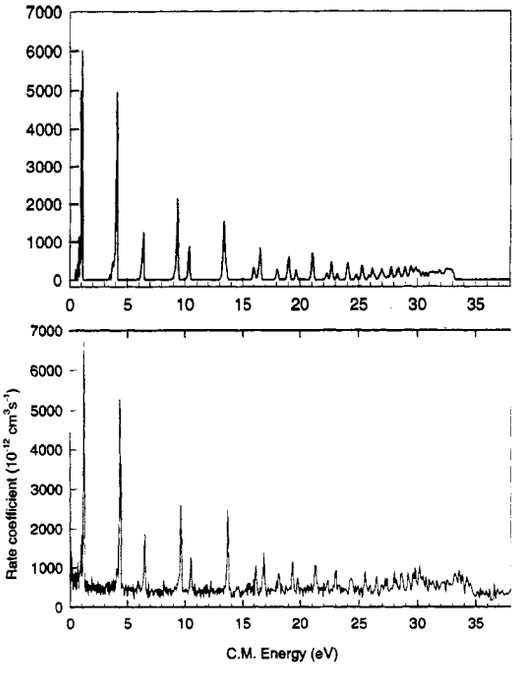

Fig. 2. Recombination rate coefficient for Ar^{15+} *vs.* relative energy. The upper figure represent the calculated spectrum (folded with 20 meV/k_B transverse temperature and 0.13 meV/k_B longitudinal temperature) and the lower figure shows the measured data.

The correction for the drag force on the ions was checked by saw-tooth scans of the electron velocity. In Fig. 1 (middle) the detuning of the cathode voltage from cooling is shown. The lower part of this figure displays the corresponding CM energies for the case of Ar^{15+}. At the top the four spectra are displayed (which should be identical in the CM system); two where the electrons moved faster and two where they move slower then the ions. With the inclusion of a correction for the drag force acceleration into the relativistic transformation from laboratory into CM system an agreement of the four spectra to better then 10 meV was possible. This gives an estimate of the systematic error in the energies.

3. Results and Discussion

The results from the DR resonances with Ar^{15+} after transformation into CM energies and corrections for space-charge effects and drag force are summarized in the lower part of Fig. 2. The upper part of Fig. 2 shows the theoretical cross sections folded with the electron beam temperatures (20 meV/k_B transverse temperature and 0.13 meV/k_B longitudinal temperature) . The cross sections are calculated in isolated resonance approximation, using the AUTOSTRUCTURE code [22]. The calculations are based on the many-body Breit–Pauli approximation for the wavefunctions in intermediate coupling for low n and the high n states are obtained by extrapolating radial wavefunctions assuming quantum defect theory.

The spectra show the Rydberg series of doubly excited states formed by $\Delta n = 0$ DR transitions in Ar^{14+}. The theory predicts that two series, $1s^22s_{1/2}$ to $1s^22p_{1/2}(nl)$ and $1s^22p_{3/2}(nl)$ with $n \geqslant 10$, are seen. A labelling of some of the main resonances is given in Fig. 3. The theoretical and experimental line positions and rate coefficients compare rather well. In the spectrum one can identify Rydberg states up to $n = 23$ for the $1s^22p_{3/2}$ core excitation. For calculating the Rydberg series $n_{max} = 43$ was chosen (see above) and the positions of the series limits and the rates in this range of very high n are quite well in accord. A possible influence of an external field would become visible in this range of n as it was probably the case in Ref. [23]. The data is well compatible with zero external field strength.

A more detailed comparison of the data with calculated resonances is shown in Fig. 3. up to the $1s^22p_{3/2}(12\ell)$ resonance, overlapping with $1s^22p_{1/2}(13\ell)$ in the last peak. The fluctuation in the difference between calculated and measured resonance positions is outside the experimental error bars and shows the limitations of this kind of calculation. It varies with n and ℓ in the Rydberg state. The shoulder from the $1s^22p_{1/2}(13\ell)$ resonance is in theory on the right side and in the experimental data on the left side of the $1s^22p_{3/2}(12\ell)$ resonance (as labelled in Fig. 3). In the data

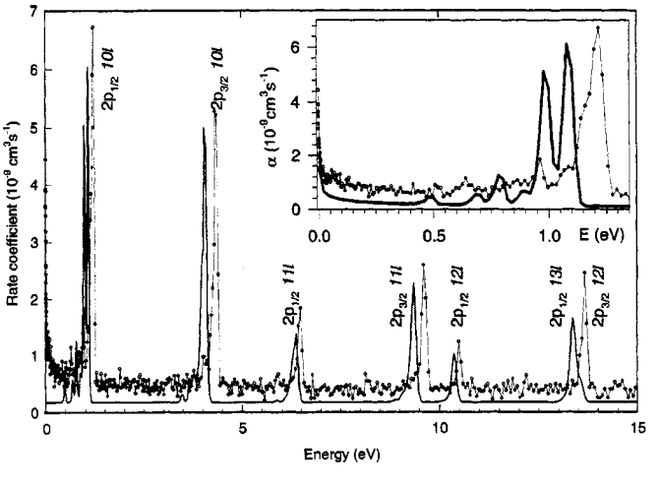

Fig. 3. Comparison of measured (connected points) and calculated (full line) recombination rates for Ar^{15+} in an expanded energy range with labelling of the doubly excited states (see text). The insert shows the comparison for the $1s^22p_{1/2}(nl)$ doubly excited states only.

one sees clearly the $1s^2 2p_{1/2}(10s)$ and (10p) resonances resolved and separated from the higher ℓ. On the insert of Fig. 3 the $2p_{1/2}(10\ell)$ series only is shown. In the experimental data, the 10s resonance is at 0.65 eV, the 10p resonance group is at around 0.95 eV, and the 10d resonance group starts at around 1.1 eV. The rest of the series converges in a large peak at around 1.2 eV. The difference between the calculated and the experimental resonance position increases with decreasing ℓ. There seems to be also a slight difference in the fine structure splitting. This is, however, not surprising considering the simplicity of the calculation in which correlation and relativistic effects were treated in low order and quantum electrodynamical corrections were not included. A detailed calculation, however only for $n = 10$ of the Rydberg series, is presented in Ref. [26]. For the CM energy approaching zero, the experimental rate rises sharply. This rise, which is not predicted by the DR calculation, could be interpreted to be due to radiative recombination. On the insert of Fig. 3 the radiative radiation rate has been added to the DR rates. It was calculated according to Ref. [26]. with $Z_{\text{eff}} = 15$ verified in Ref. [17] with the same electron temperatures as used for the DR rates. The experimental rate under cooling is $4.5 \cdot 10^{-9}\,\text{cm}^3\,\text{s}^{-1}$. The RR prediction peaks at $1.47 \cdot 10^{-9}\,\text{cm}^3\,\text{s}^{-1}$ which is around a factor of 3 below the experimental rate (see discussion in the introduction).

The DR cross seection for ground state He-like ions results predominantly from radiative stabilization of lithium-like doubly excited states $1s2s(^{1,3}S)nl$ and $1s2p(^{1,3}P)nl$. A comparison of the measured DR resonances in C^{3+} with the AUTOSTRUCTURE calculation [22] (folded with $10\,\text{meV}/k_B$ transverse temperature and 0.15 meV longitudinal temperature) is shown in Fig. 4. The agreement is reasonable. With the almost an order of magnitude better resolution than the experiment of Kilgus *et al.* [5], one sees, however, now a discrepancy between the calculated and measured line positions for the $1s2l2l'$ and $1s2l3l'$ resonances at around 240 eV and around 280 eV, respectively. A system, such as doubly excited C^{3+} with three open shells, places quite some challenge on atomic structure calculations even with only three electrons being involved. Correlations are getting very important in treating the $1s2l2l'$ and $1s2l3l'$ resonances. This becomes obvious at the small peak seen just above 227 eV. It is from the $1s2s^2(^2S)$ resonance. This resonance state has no allowed radiative decay channel and should not appear in a DR spectrum. Due to correlation, which mixes this state with the $1s2p^2(^2S)$ state, a finite radiative width is obtained. The intensity of this resonance is quite well described by the AUTOSTRUCTURE calculation, the energy is, however, shifted by more then 1 eV. At high n, where correlation is reduced, the agreement becomes increasingly better, and is quite perfect at the series limit. A more elaborate calculation which treats correlation to higher orders gives also perfect agreement for the line positions in the low n region [8].

Near the series limit another "mixing effect" occurs. The stabilizing radiative decay which mainly determines the DR cross section should be strongest for the $1s^2(^1S)nl$ to $1s2p(^1P)nl$ transition for high n. However, in the case of C^{3+} the cross section for the ^1P nl series is reduced for $n \geqslant 7$ considerably due to autoionization into other channels with lower excitation threshold, as discussed in Ref. [5, 8].

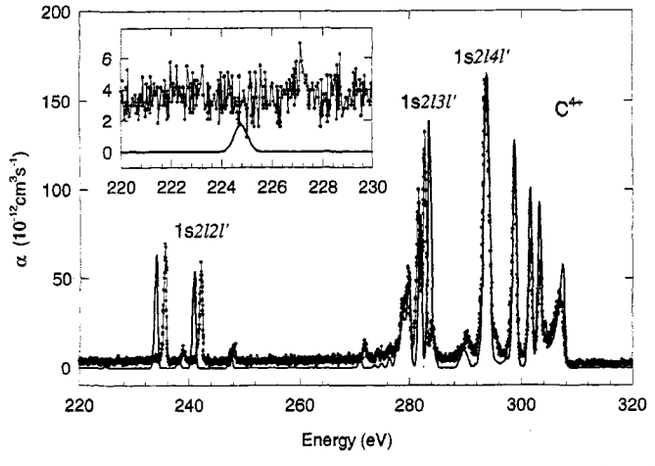

Fig. 4. Recombination rate coefficient for C^{4+} *vs.* relative energy. The calculated spectrum (full line) is folded with $10\,\text{meV}/k_B$ transverse temperature and $0.15\,\text{meV}/k_B$ longitudinal temperature (labelling for groups of doubly excited states). The insert (same scales as main figure) shows the region of the $1s2s^2(^2S)$ resonance (at 225 eV and 227 eV).

4. Conclusion

We have shown that electron-ion collision reactions can be studied with high resolution in CRYRING by using energetic stored ion beams and an expanded electron beam for cooling and as a target. For bare ions of charge 14 and Li-like Ar, the experimentally observed rate coefficient is enhanced by a factor of 3 as compared to radiative recombination near zero relative energy. The explanation of this effect with three-body recombination models awaits further evidences.

It was shown that dielectronic recombination resonances can be measured with an accuracy in the order of up to 10^{-2} eV. Here the results are compared with an isolated resonance model calculated in multi-configuration Breit–Pauli approximation. It is found in reasonable good agreement with the data but shows some discrepancy in the energy positions of the low-lying dielectronic recombination resonances due to a restricted treatment of electron correlation.

Acknowledgements

The authors would like to thank the staff of CRYRING for their assistance during this experiment. This work was supported by the Swedish Natural Science Research Council (NFR) and the Knut and Alice Wallenberg Foundation.

References

1. Schuch, R., in "Large Facilities in Physics" (Edited by M. Jacob and H. Schopper) (World Scientific Publishing Co. 1995), p. 222.
2. Burgess, A., Astrophys. J. **139**, 776 (1964); **141**, 1588 (1965).
3. Dubau, J. and Volonté, S., Rep. Prog. Phys. **43**, 199 (1980).
4. Spies, W. *et al.*, Phys. Rev. Lett. **69**, 2768 (1992).
5. Kilgus, G. *et al.*, Phys. Rev. **A47**, 4859 (1993).
6. DeWitt, D. R. *et al.*, Phys. Rev. **A50**, 1257 (1994); DeWitt, D. R. *et al.*, Phys. **B28**, L147 (1995); DeWitt, D. R. *et al.*, Phys. Rev. **A53**, 2327 (1996).
7. Schmidt, H. T. *et al.*, Phys. Rev. Lett. **72**, 1616 (1994).
8. Mannervik, S. *et al.*, Phys. Rev. A. **55**, 1810 (1997).
9. Stobbe, M., Ann. Phys. (Leipzig) **7**, 661 (1930).

10. Bates, D. R., Kingston, A. E. and McWhirter, R. W. P., Proc. Roy. Soc. **A267**, 297 (1962).
11. Schuch, R. *et al.*, Nucl. Instr. Meth. **B79**, 59 (1993).
12. Quinteros, T. *et al.*, Phys. Rev. **A51**, 1340 (1995).
13. Gao, H. *et al.*, Phys. Rev. **A54**, 3005 (1996).
14. Wolf, A. *et al.*, Z. Phys. **D21**, 69 (1991).
15. Müller, A. *et al.*, Physica Scripta **T37**, 62 (1991).
16. Gao, H. *et al.*, submitted to J. Phys. B.
17. Frank, A. *et al.*, AIP Conference Proceedings 274, p. 532, HCI Manhattan Ks. (1992) (Edited by P. Richard, M. Stoeckli, C. L. Cocke and C. D. Lin) (New York, AIP 1993).
18. Gao, H. *et al.*, Phys. Phys. Rev. Lett. **75**, 4381 (1996).
19. Uwira, O. *et al.*, Hyperfine Interaction **108**, 167 (1997).
20. Baird, S. *et al.*, Phys. Lett. **B361**, 184 (1995).
21. Hahn, Y. and Krstic, P., J. Phys. B: At. Mol. Opt. Phys. **27**, L509 (1994).
22. Badnell, N. and Pindzola, M. S., Phys. Rev. **A39**, 1685 (1989).
23. Schenach, S. *et al.*, GSI preprint 94-5 (1994); Z. Phys. **D30**, 291 (1994).
24. Danared, H. *et al.*, Phys. Rev. Lett. **72**, 3775 (1994).
25. Schuch, R. *et al.*, Hyperfine Interactions **99**, 317 (1996).
26. Zong, W., Schuch, R., DeWitt, D. R., Lindroth, E. and Gao, H., Phys. Rev. A. in print.